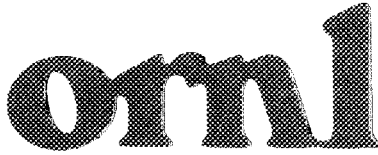


MARTIN MARIETTA ENERGY SYSTEMS LIBRARIES



3 4456 0333846 7

ORNL/TM-11819



OAK RIDGE
NATIONAL
LABORATORY



Thermal Energy Storage
Technical Progress Report
April 1989–March 1990

J. J. Tomlinson

OAK RIDGE NATIONAL LABORATORY
CENTRAL RESEARCH LIBRARY
CIRCULATION SECTION
4300N ROOM 175
LIBRARY LOAN COPY
DO NOT TRANSFER TO ANOTHER PERSON
If you wish someone else to see this
report, send in name with report and
the library will arrange a loan.

MANAGED BY
MARTIN MARIETTA ENERGY SYSTEMS, INC.
FOR THE UNITED STATES
DEPARTMENT OF ENERGY

This report has been reproduced exactly from the best available copy.

Available to DOE and DOE contractors from the Office of Scientific and Technical Information, P.O. Box 62, Oak Ridge, TN 37831, prices available from (615) 576-8401, FTS 626 8401.

Available to the public from the National Technical Information Service, U.S. Department of Commerce, 5285 Port Royal Rd., Springfield, VA 22161.

This report was prepared as an account of work sponsored by an agency of the United States Government. Neither the United States Government nor any agency thereof, nor any of their employees, makes any warranty, express or implied, or assumes any legal liability or responsibility for the accuracy, completeness, or usefulness of any information, apparatus, product, or process disclosed, or represents that its use would not infringe privately owned rights. Reference herein to any specific commercial product, process, or service by trade name, trademark, manufacturer, or otherwise, does not necessarily constitute or imply its endorsement, recommendation, or favoring by the United States Government or any agency thereof. The views and opinions of authors expressed herein do not necessarily state or reflect those of the United States Government or any agency thereof.

ORNL/TM-11819
Dist. Category UC-202

ENGINEERING TECHNOLOGY DIVISION

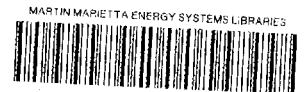
**THERMAL ENERGY STORAGE TECHNICAL PROGRESS REPORT
APRIL 1989 - MARCH 1990**

J. J. Tomlinson

Date Published - March 1991

Prepared for
Office of Renewable Energy
AI 10 01 00 0

Prepared by the
OAK RIDGE NATIONAL LABORATORY
Oak Ridge, Tennessee 37831-6285
managed by
MARTIN MARIETTA ENERGY SYSTEMS, INC.
for the
U.S. DEPARTMENT OF ENERGY
under contract DE-AC05-84OR21400



3 4456 0333846 7

CONTENTS

LIST OF FIGURES	v
LIST OF TABLES	vii
ABSTRACT	1
1. PROGRAM OVERVIEW	1
1.1 DIURNAL TES PROGRAM	2
1.2 INDUSTRIAL TES PROGRAM	5
2. TECHNICAL PROGRAM - DIURNAL TES	7
2.1 DEVELOPMENT OF COMPLEX COMPOUND CHILL STORAGE SYSTEM	7
2.1.1 Preconditioning of the Complex Compound	10
2.1.2 Heat Exchanger Loading Density	10
2.1.3 Heat Rejection and Approach Temperatures	12
2.1.4 Operating Modes	12
2.1.5 Bench-scale Demonstration	14
2.2 ASSESSMENT OF PCM WALLBOARD	17
2.2.1 PCM Wallboard Subroutine Validation	17
2.2.2 Solar Ray Tracing Subroutine Validation	17
2.2.3 Simulation of Building with PCM Wallboard	18
2.2.4 Economic Analysis	21
2.2.5 PCM Wallboard Cost	24
2.3 PCM WALLBOARD DEVELOPMENT	27
2.3.1 Progress with Fire Safety	28
2.3.1 Alternative Methods for PCM Incorporation	29
2.4 EFFECT OF DOPANTS ON SOLID-STATE PCMS	30
2.5 DIRECT CONTACT ICE STORAGE SYSTEM DEVELOPMENT	32
2.6 DEVELOPMENT OF SEPARATION TECHNIQUES FOR A DIRECT CONTACT ICE STORAGE SYSTEM	35
2.6.1 Membrane Evaluation	35
2.6.2 Mechanical Separator Evaluation	35
2.6.3 Ranque - Hilsch Vortex Tube	36

3. TECHNICAL PROGRAM - INDUSTRIAL TES	37
3.1 DEVELOPMENT/TESTING OF TES MEDIA FOR INDUSTRIAL APPLICATIONS	37
3.2 DEVELOPMENT OF DIRECT CONTACT MOLTEN SALT/AIR HEAT EXCHANGER	38
4. CONCLUSIONS	41
REFERENCES	43

LIST OF FIGURES

<u>Figure</u>	<u>Page</u>
1 Equilibrium phase behavior for complex compound system	8
2 Reaction rates and coordination sphere utilization with various complex compound conditioning. Data are for adsorptions in CC180-1580 at 45°C with a 6°C approach temperature	11
3 Useable mole number change for CC180-1580 with 6°C approach temperature	11
4 Cost of reactor internals and vessels for TES using CC180-1580	13
5 Coordination sphere utilization as a function of approach temperature for CC180-1580 at a heat rejection temperature of 95°F	13
6 Coordination sphere utilization as a function of heat rejection temperature for CC180-1580 at an approach temperature of 16°C	15
7 Comparison of constant rate and constant pressure adsorptions of CC180-1580 at 45°C. Maximum approach temperature is 6°C	15
8 Adsorption rates (at 35°C) for lab-scale system (0.002 ton-h) and bench-scale system (1 ton-h)	16
9 Desorption rates (at 35°C) for lab-scale system (0.002 ton-h) and bench-scale system (1 ton-h)	16
10 PCM system allowable cost with electricity backup as function of period and latent heat capacity	25
11 Direct contact ice system schematic (2½ ton-h nominal capacity)	34
12 Schematic of proposed high temperature TES test facility	39

LIST OF TABLES

<u>Table</u>	<u>Page</u>
1 Wallboard thermal characteristics	19
2 Total energy use summary	20
3 Supplemental heating system data	21
4 PVES (\$) of PCM addition to walls of 1800-ft ² home in Denver; 200 ft ² of south-facing glazing; no window insulation	23
5 PCM wallboard characteristics for 5040 ft ² of ½-in. plasterboard; PCM latent storage capacity measured to be 83 Btu/lb	24
6 Refrigerant molar volumes at 32° F	33

**THERMAL ENERGY STORAGE TECHNICAL PROGRESS REPORT
APRIL 1989 - MARCH 1990**

J. J. Tomlinson

ABSTRACT

The Department of Energy (DOE) is supporting development of thermal energy storage (TES) as a means of efficiently coupling energy supplies to variable heating or cooling demands. Uses of TES include electrical demand-side management in buildings and industry, extending the utilization of renewable energy resources such as solar, and recovery of waste heat from periodic industrial processes. Technical progress in development of TES for specific diurnal and industrial applications under Oak Ridge National Laboratory's TES program from April 1989 to March 1990 is reported.

1. PROGRAM OVERVIEW

Thermal energy storage consists of a range of technologies that allow an energy supply to be coupled to a heating or cooling demand. Acting as a buffer, TES facilitates the use of a time-varying energy resource to meet a constant or variable demand for heat or cool. Alternatively, TES is used to store available energy as sensible or latent heat in a material to meet an energy demand occurring at a later time. There are several advantages afforded by the use of TES including: (1) reduced sizes for heating and cooling systems in buildings, (2) load management of electricity used for heating and cooling, (3) waste heat utilization, and (4) renewable energy use.

Reduced heating/cooling system sizes. Building space conditioning systems are typically sized to meet peak heating and cooling conditions. Consequently, these systems are oversized for most of the time and operate at reduced capacity. A TES system coupled to smaller heating/cooling plants that are operated continuously can meet a thermal demand that is much larger than the installed capacity. The overall result is a smaller and less costly heating/cooling system that operates most of the time at its most efficient rating. This feature can also be useful when a heating or cooling load increases (e.g., during building expansion); TES increases the duty cycle of the existing space conditioning system so that the larger peak thermal load can be met with no increase in installed capacity.

Electric load management. Thermal energy storage allows one to schedule electricity usage patterns. This TES feature can be an advantage to a customer to avoid on-peak electricity costs as well as to the electrical utility who is interested in shifting load from certain times of the day. Due to commercial air conditioning, utilities generally are experiencing major load growth, particularly in the summer. To encourage a shift from summer peak periods, utilities have instituted a variety of incentive programs. Examples include cash rebates that are proportional to the capacity shifted by a customer and support for studies to determine the feasibility of TES for a specific application or customer. These incentives add to customers savings in demand charges to make a strong climate for further growth in cool storage. At the present time, there are over 1,000 cool storage systems now operating in the United States. Heat storage often appears a viable option for off-peak building heating particularly in areas where the electrical demand due to heating is high as is generally the case in the northeastern United States.

Waste heat utilization. In many industries, process heat is required at a time that does not coincide with the availability of waste heat. Particularly in high temperature batch processing, as in ceramics manufacturing, waste heat exhausted in flue gas could be stored in a material and reused at a later time for drying or for preheating operations. The result is an overall reduction in the energy requirements of the industry and a reduction in thermal emissions from the plant.

Renewable energy use. Solar energy used for building heating typically requires the presence of a TES system since the heat must be delivered on a diurnal basis at times when the solar flux is reduced or absent. With a TES system operated through one cycle annually, the winter chill resource could be used for space cooling during the summertime.

1.1 DIURNAL TES PROGRAM

A primary target of the diurnal TES program is the development of a chill storage system that can be used to provide on-peak refrigeration in the -40°F to $+20^{\circ}\text{F}$ range. All refrigerated warehouses, food processing, and many chemical processing plants use refrigeration in this temperature range. A chill storage system allows the compressor load to be removed from the electrical on-peak period and cooling to be provided either continuously or on a schedule and at a rate that is controlled by the process or storage conditions. Rocky Research, a relatively

small research and development company, is working to develop a chill TES system based on the use of ammonia and an ammoniated salt. During the TES charging process, ammonia desorbed from the salt by compressor operation is condensed and stored in a refrigerant receiver. During the discharging process, the refrigerant is evaporated by heat from the cooling load and is returned to combine with the salt. The discharge process proceeds without compressor operation. The fact that the chill TES system uses ammonia is a key advantage since ammonia refrigerant is commonly used in industrial refrigeration systems. Details of recent technical results in this project are described in Section 2.1.

A second major initiative is the development of building materials with enhanced heat capacity. Although early techniques for using containerized phase change materials (PCMs) in buildings have been examined, commercialization of these concepts have foundered due to the added expense of engineering them into standard structures, or in the case of latent heat storage in some PCMs, stability problems. One method proposed for overcoming these problems uses a stable PCM incorporated directly into standard gypsum wallboard. Research on suitable PCMs and methods to contain them in the interstices of gypsum has been continued by the program at the University of Dayton Research Institute.¹ In the previous reporting period,² a suitable PCM in the form of a paraffin blend was chosen, and an immersion facility was constructed at Oak Ridge National Laboratory (ORNL) for imbibing the melted PCM into full-sized sheets of wallboard. The paraffin blend with n-octadecane as the main constituent melts and freezes sharply around 72°F satisfying the requirement of a PCM in the comfort zone temperatures of 65°-75°F. A process for incorporating the PCM into wallboard has been studied, and full-size sheets of PCM wallboard have been produced for testing. Details of recent experimental work in this project are given in Section 2.3.

The development of PCM wallboard has continued under the assumption that it can provide economic benefits to the consumer which outweigh its implementation costs. These benefits include the following:

1. Reduced heating costs associated with solar energy stored in the PCM during the day and released at night.

2. Reduced heater cycling due to moderation of temperature swings through the use of a PCM with a large surface area.
3. Increased thermal comfort due to the PCM absorbing and releasing energy at its transition temperature.³

Item 1 above applies to solar houses where direct beam radiation passing through a window could be used to heat the surface of the PCM wallboard thereby transferring energy to the PCM. Item 2 proposes reduced costs associated with running a furnace longer at its highest efficiency to charge the PCM, and item 3 deserves attention as an added benefit provided by PCM wallboard. To address item 1, an assessment was performed with the objective of determining the economic benefit of the PCM wallboard in a small residential building and the optimal PCM content. The results of this study are reported in Section 2.2.

In addition to latent heat storage through freezing and melting of a PCM, latent heat can be stored and released through crystallographic changes in a solid material. As companion research to the PCM wallboard study using paraffin, the University of Nevada - Reno is engaged in a research project to understand and describe solid-solid transitions that occur in certain polyalcohol systems. Based on this understanding, dopants were identified and added to a material with a high solid-solid transition temperature to lower this transition to the room temperature range without a disproportionate loss in the heat of transition. Results of this work to date are reported in Section 2.4.

A third major program initiative is the development of an advanced TES system for building cooling. Cool storage using ice is growing as a means of meeting a building cooling load using off-peak electricity. In conventional systems, ice is frozen to an evaporator surface and must either be removed to be useful or is slowly melted away from the heat exchange surface during discharge. In the case of dynamic ice making, the ice is defrosted from the surface heat exchanger. This requires a defrost mechanism and extra energy for defrosting. In systems where the ice remains frozen to a surface during discharge, large, extended surface heat exchangers are required to keep approach temperatures relatively small. Direct contact between an evaporating refrigerant and water is one method for increasing the heat transfer rate and eliminating the need for a heat transfer surface. Research is underway at CBI Industries to develop a direct contact system and to measure its performance. The system is operated by

sparging evaporating refrigerant against a stream of water. Ice crystals fall into a tank, and the refrigerant vapor returns to the compressor. The water carryover issue is being accommodated by CBI by using a new compressor technology unique to the cooling application. Supporting work is underway at North Carolina A&T State University to measure this water carryover and to develop effective methods of reducing carryover so that conventional compressor technologies may be used in conjunction with the direct contact process. This work, just begun, is reported in Section 2.6.

1.2 INDUSTRIAL TES

Industrial TES consists of technologies used to capture available waste heat for reuse in an industrial process. For several years, the industrial TES program has continued development of a composite TES material that, as pellets, could be used in a packed bed regenerator. The material, a composite consisting of a ceramic matrix suffused with a eutectic PCM, was carried through laboratory development by the Institute of Gas Technology in prior years.⁴ Later analytical studies on the predicted performance of a packed bed of composite material were conducted by Mississippi State University (MSU). To verify and calibrate the packed bed model and to determine the lifetime of the composite, thermal/hydraulic tests of a packed bed using flue gas for charging and air for discharging are being planned for execution by MSU. Progress in this work is described in Section 3.1.

Studies of direct contact heat transfer between a molten salt and air as a potential means of heat transfer in a solar thermal application were initiated in prior years by the Solar Energy Research Institute (SERI). Although not directly applicable to TES, these studies were deemed supportive to the overall TES program; therefore, support was given to complete these experimental studies. An existing direct contact molten salt/air loop at SERI was used to determine the significance of thermal radiation on the overall heat exchange effectiveness of a packed bed heat exchanger. The final results from this study are presented in Section 3.2.

2. TECHNICAL PROGRAMS - DIURNAL THERMAL ENERGY STORAGE

2.1 DEVELOPMENT OF COMPLEX-COMPOUND CHILL STORAGE SYSTEM

Although the concept of a low temperature TES system based on the use of complex compounds to store energy as heats of reactions has been described in detail in earlier progress reports,^{1,2} a simple review of the system is helpful in understanding the processes and technical issues which were addressed in the current reporting period. The principal components of the system are two containers; one contains liquid ammonia with a free surface, and the other contains a salt that can take up ammonia by chemisorption. At the same temperature, equilibrium vapor pressure of the ammoniated salt with ammonia as the ligand is significantly lower than the saturated vapor pressure of ammonia as shown in Fig. 1. The TES system is charged and discharged by transferring ammonia between the two containers and exploiting the heats of vaporization and sorption of ammonia. During the adsorption of ammonia by the salt, heat is released and must be carried from the system; the desorption process is endothermic. For a successful system, the heat and mass exchange inside the salt container must be efficient and done cost effectively. In the prior reporting period,² studies were initiated on three technologies designed to enhance heat and mass exchange efficiency between the solid salt and ammonia vapor: a slurry concept, a carrier liquid concept, and the more conventional dry bed reactor or surface heat exchanger. This research proved the dry bed system to be the only viable option for the following reasons:

1. Cost. Economic considerations indicated that the dry bed concept would be less expensive than the alternatives studied. The projected cost for a complete dry bed system excluding installation is about \$57/kWh (\$200/ton-h) with about 36% of this cost attributed to the heat exchanger. Heat exchanger cost for the slurry and carrier liquid concepts was estimated to be about \$24/kWh (\$85/ton-h). Additionally, the balance-of-system costs were expected to be higher for both the slurry and carrier liquid concepts than for the dry bed system. In the case of the slurry concept, slurry pumps and distribution systems would be required. The carrier liquid system would require a solution pump along with a solid-liquid phase separation system (e.g., membranes).

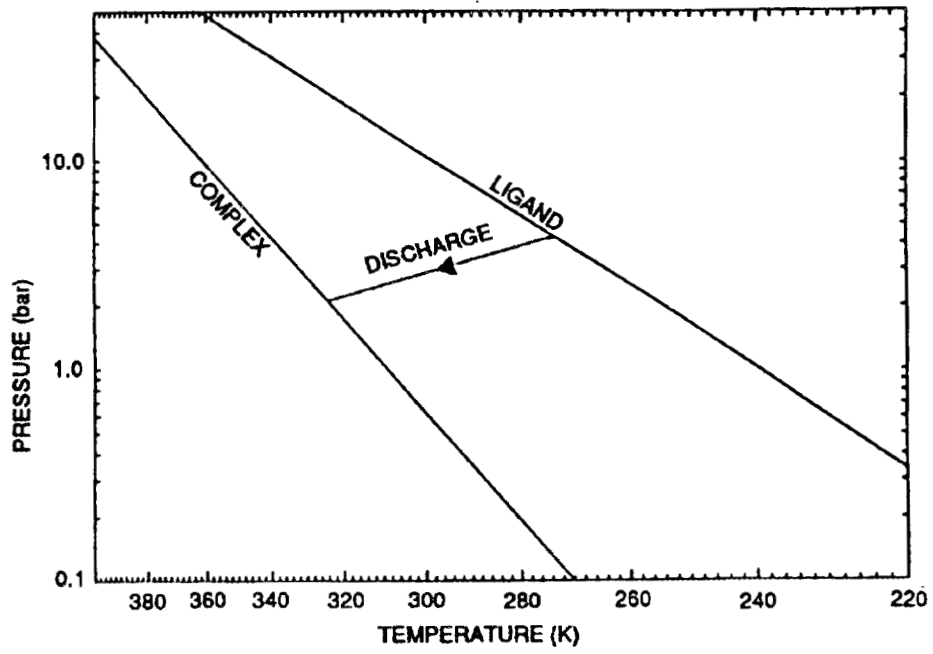


Fig. 1. Equilibrium phase behavior for complex compound system.

2. Development Risk. The dry bed system is straightforward and simple. Therefore, the risk of developing a working dry bed system is very low. The main issue is developing a dry bed system that meets the technical and cost goals established. Technical risks were deemed high in the case of both the slurry and carrier liquid concepts. In these systems, there were major concerns in finding appropriate carrier liquids which are proven to be stable in the presence of ammonia and the salt, or, in the case of the slurry system, materials compatibility and wear in slurry pumps.
3. Integration with refrigeration systems. Since the salt remains fixed as a solid in the reactor tank, the dry bed concept can be easily integrated into an ammonia cooling system without ammonia contamination and salt carryover into the refrigeration system. The carrier solvent and slurry system would require fluids that minimize carryover into the vapor compression system or would require process isolation with heat exchangers. This results in increased cost and elevated approach temperatures.
4. Simplicity and reliability. With no moving parts, the dry bed system should prove to be very reliable. The carrier solvent and slurry systems would require periodic maintenance and replacement of pumps.
5. Industry preference. The three different concepts for a complex compound chill storage system were discussed with refrigeration equipment manufacturers and experts with refrigeration systems. It was generally noted that a dry bed reactor development would be the one most acceptable to both manufacturers and users.

On this basis, further research was conducted in the reporting period on the dry bed concept. The research consisted of experiments to determine promising heat exchanger designs and to demonstrate the performance of a working system on a scale larger than the earlier bench-scale studies. Issues addressed included quantification of the capacity of the salt to complex with ammonia as a function of heat rejection temperature, salt loading density, and other factors that affect the storage capacity of the compound.

2.1.1 Preconditioning of the Complex Compound

Early in the investigation of the dry bed system, it became apparent that the manner in which the initial adsorption was conducted had a major effect on salt utilization. Rapid initial adsorptions were required for proper utilization of the coordination sphere that surrounds each salt molecule. Specifications for preconditioning were developed which resulted in repeatable coordination sphere utilization. It was also discovered that saturation of the complex compound with refrigerant for a period of time resulted in superior conditioning. Figure 2 shows reaction rates and mole number change (ΔN) without preconditioning, with preconditioning in which the rate of initial adsorption is controlled, and with soak preconditioning. The reaction rate is stated in terms of moles_{ammonia}/moles_{salt}/h. The initial adsorption for the bench-scale system constructed earlier is shown as line 2 in Fig. 2. It can be seen that the useable portion of the coordination sphere increases to about 85% following soak preconditioning. This represents a process that will occur automatically during installation of a TES system. The salt will be ammoniated immediately following reactor assembly to provide mechanical stability to the salt load. The interval of time between reactor assembly and actual operation will constitute a soak period.

2.1.2 Heat Exchanger Loading Density

The quantity of ammonia participating in adsorption and desorption decreases as the packing density of the complex in the heat exchanger is increased. The results of laboratory-scale experiments with the salt CC180-1580 at two loading densities are illustrated in Fig. 3. The general trend shows that the refrigerant holding capacity increases at lower loading densities. However, lower loading densities require more heat exchange surface and a larger container so that the most economic system may not be the one with the least salt. Figure 4 which shows normalized reactor costs for the data from Fig. 3 illustrates this point. The lower densities increase the refrigerant holding capacity; however, they also result in an increased cost per unit of storage capacity. The cost data used in Fig. 3 consist of a salt cost of \$0.91/lb and a reactor (heat exchanger and associated internals, vessel and labor) of \$2.03/ft³ of complex compound in the reactor. These costs are based on estimates and vendor quotes for the materials and construction. Although the data are preliminary, it is clear that the loading density of salt should

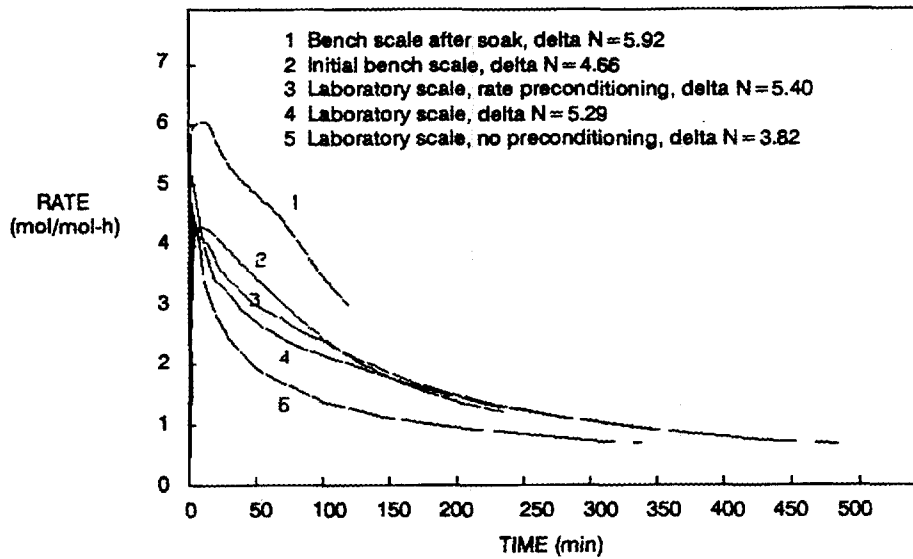


Fig. 2. Reaction rates and coordination sphere utilization with various complex compound conditioning. Data are for adsorptions in CC180-1580 at 45°C with 6°C approach temperature.

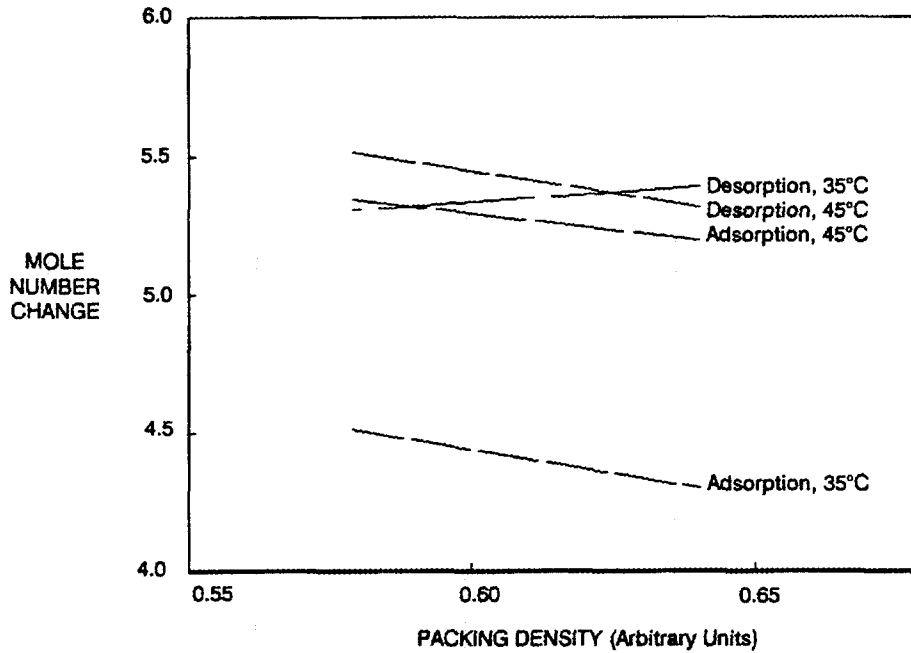


Fig. 3. Useable mole number change for CC180-1580 with 6°C approach temperature.

not be decreased to improve coordination sphere utilization. Improving the loading density beyond a certain point is not practical due to mechanical considerations.

2.1.3 Heat Rejection and Approach Temperatures

The amount of ammonia that can be adsorbed and desorbed cyclically in a TES system depends on the heat rejection temperature and approach temperature. Figure 5 shows the useable coordination range for the adsorption and desorption processes as a function of approach temperature. The solid lines are least-square fits to the sorption data. It is obvious that decreasing approach temperatures consistently result in smaller storage utilization. These data describe sorption at 95°F (35°C); higher heat rejection temperatures result in better utilization of the ammonia as shown in Fig. 6. The storage temperature to be maintained determines the approach temperature. An approach temperature of 4°C will allow -28°C refrigeration with the salt CC180-1580. Figure 5 indicates that the minimum utilization of ammonia is 5.18 moles of ammonia per mole of salt with greater utilization at higher reject temperatures or approach temperatures.

2.1.4 Operating Modes

The reactivity of complex compounds is not constant over the entire coordination sphere. At fixed approach temperatures, desorptions were found to exhibit lower reaction rates as the refrigerant concentration decreases, while adsorptions showed reduced reactivity at high refrigerant loadings. The probable operating mode of TES systems is affected by this characteristic. The working media will probably be contained in a number of vessels which can be brought on line sequentially or simultaneously. Simultaneous actuation will result in a reactor capacity that is initially large as compared to the compressor or evaporator capacity. Coincident operation of several reactors will determine the system power. For most of a charge or discharge cycle in a TES system, the power at the reactors will be determined by the capacity of the compressors and condensing or evaporating conditions which will remain relatively fixed. As sorption proceeds, the capacity will be maintained by "valving in" additional reactors as the power from each decreases.

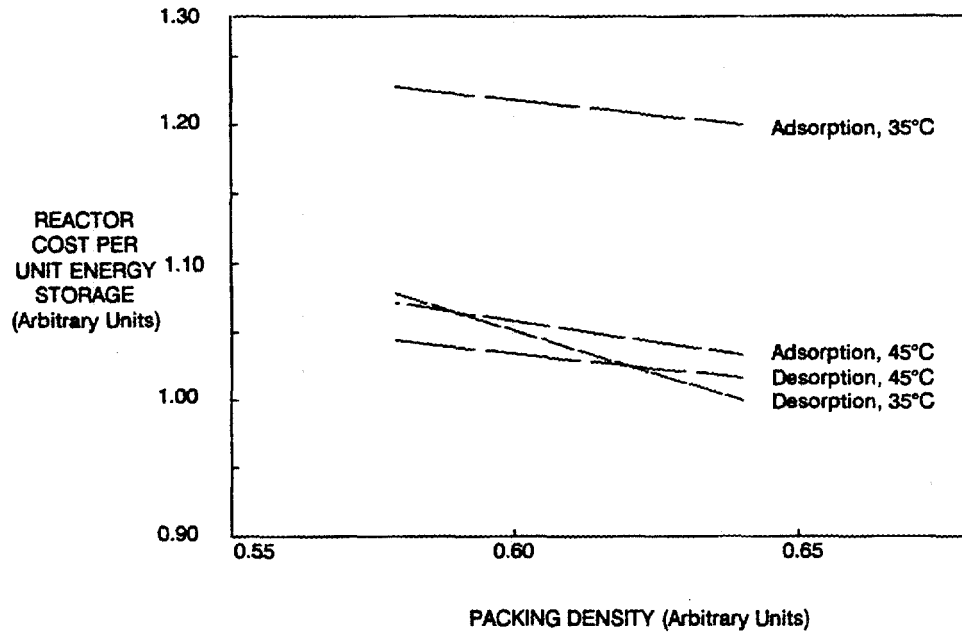


Fig. 4. Cost of reactor internals and vessels for TES using CC180-1580.

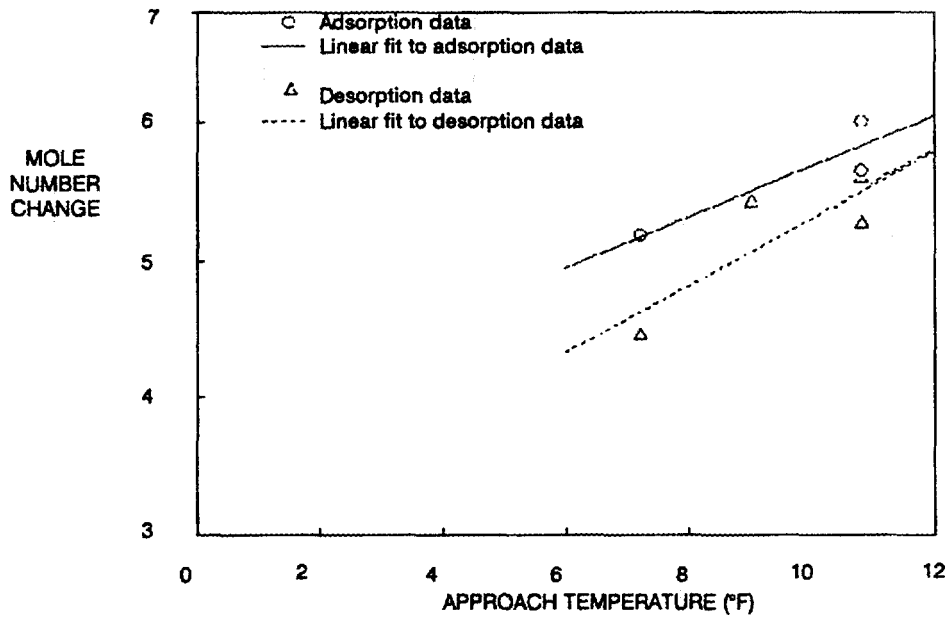


Fig. 5. Coordination sphere utilization as a function of approach temperature for CC180-1580 at a heat rejection temperature of 95°F.

Laboratory tests were conducted at constant pressure and constant reaction rate conditions to simulate these two possible operating modes. A comparison between the two modes of operation is shown in Fig. 7. In this test, the constant reaction rate condition could not be maintained (with a maximum approach temperature of 6°C) beyond 4.5 h (corresponding to a $\Delta N = 4.5$), and the adsorption was continued at constant pressure to 8 h. After 8 h, a ΔN of 5.2 moles was achieved as compared to a ΔN of 5.3 after 6 h for the constant pressure test. For a TES system that is fully charged or discharged in about 6 h, the average reaction rate must be no less than 1 mol/mol-h. It can be seen from Fig. 7 that the reaction rate falls below this target reaction rate at 4.5 h for constant reaction rate operation and at 5 h for constant pressure operation. These results show that constant pressure operation is the preferred mode of operation. A control system to bring reactors on-line sequentially may be necessary.

2.1.5 Bench-scale Demonstration

During the reporting period, the complex compound chill storage system (-28°C) was demonstrated at a scale of approximately 1 ton-h capacity. The system consisted of two reactor vessels each containing 7.9 kg of salt and an evaporator/condenser system. Instrumentation and data acquisition were provided to determine temperatures, pressures, and ammonia flow rates.

The performance of the bench-scale system proved superior to that found in earlier small-scale experiments as shown in Figs. 8 and 9. Bench-scale reaction rates and mole number changes exceeded those of laboratory-scale tests during both adsorption and desorption.

At this point, the research into the use of ammoniated complex compounds for TES has shown that these compounds are attractive for low temperature storage applications. Research is being continued to determine the long-term stability of the media, optimization of reactor hardware, development of controls, and prototype field testing.

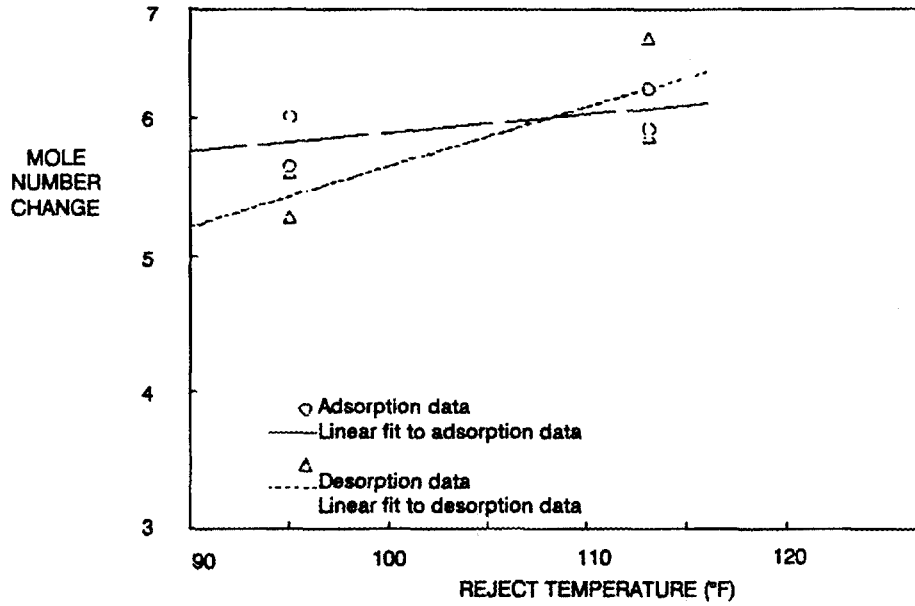


Fig. 6. Coordination sphere utilization as a function of heat rejection temperature for CC180-1580 at an approach temperature of 6°C (11°F) .

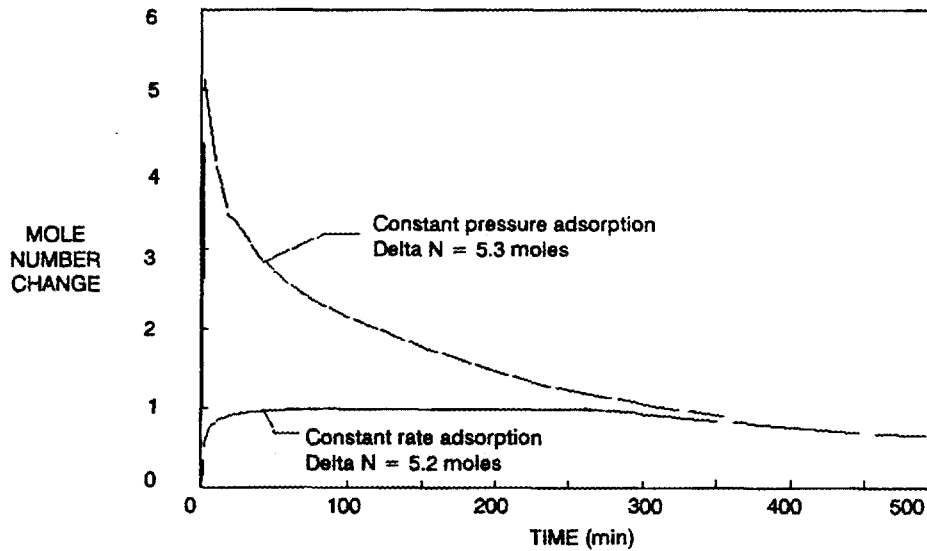


Fig. 7. Comparison of constant rate and constant pressure adsorptions of CC180-1580 at 45°C. Maximum approach temperature is 6°C (11°F).

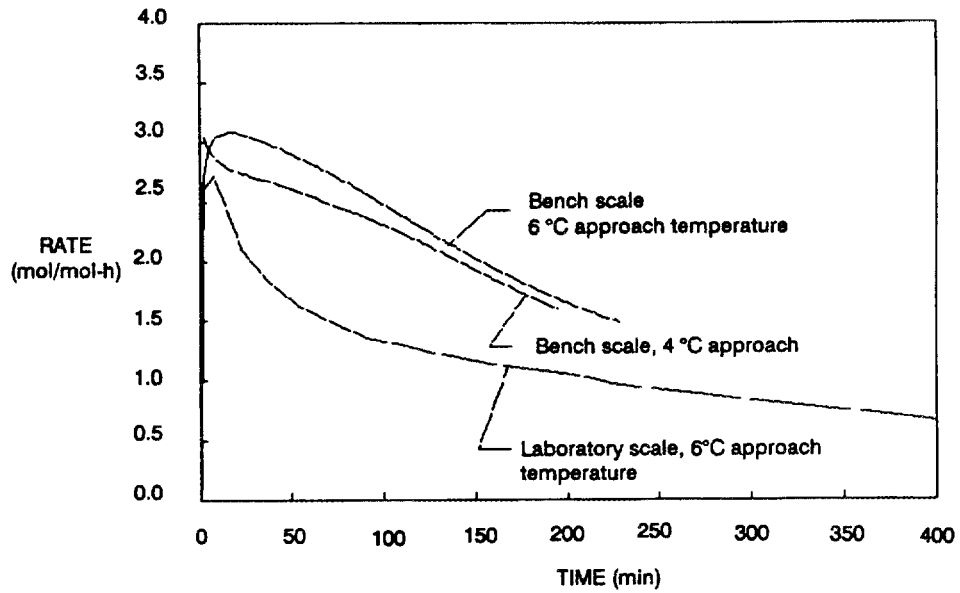


Fig. 8. Adsorption rates (at 35°C) for lab-scale system (0.002 ton-h) and bench-scale system (1 ton-h).

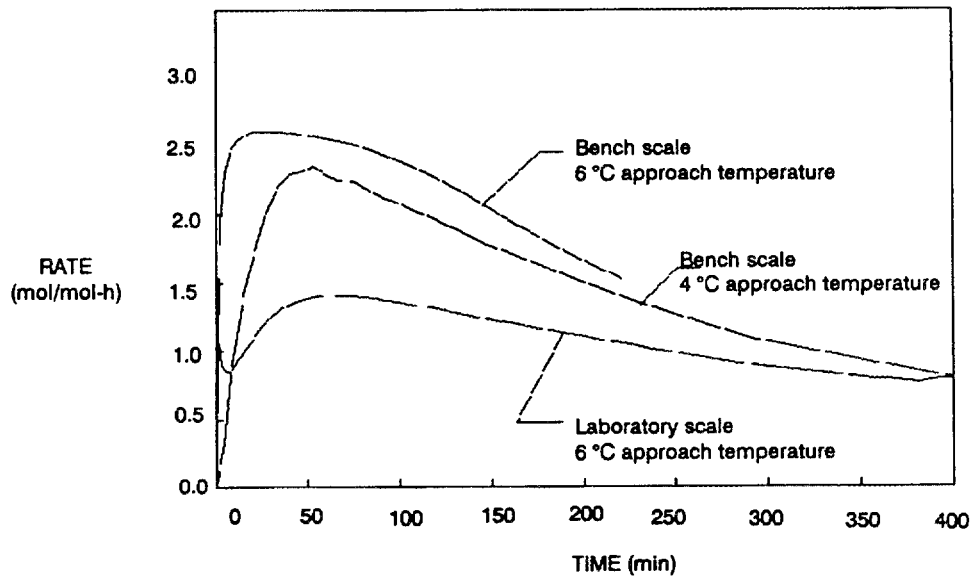


Fig. 9. Desorption rates (at 35°C) for lab-scale system (0.002 ton-h) and bench-scale system (1 ton-h).

2.2 ASSESSMENT OF PCM WALLBOARD

During the reporting period, a study was conducted to simulate the performance of a building containing PCM wallboard and to determine the allowable cost for the enhanced heat capacity material. The first step was to identify a building simulation computer code with the capacity to consider latent heat storage in the walls. After a study of available simulation tools, TRNSYS⁵ was selected for the task. Three subroutines were developed and incorporated into TRNSYS. The first accommodated latent heat storage on walls, ceiling, and floor of the building structure being simulated. A second subroutine performed solar ray tracing allowing the direct solar radiation component falling on any surface to be a function of the surface orientation and beam illumination at any time. The third subroutine modelled convective heat transfer through doorways using relations developed by Balcomb.⁶ The first two subroutines were quantitatively validated.

2.2.1 PCM Wallboard Subroutine Validation

The PCM wallboard subroutine consisted of 1-D models that characterized heat transfer normal to the exposed surface of an outside and interior wall comprised of sensible and latent heat layers. Inputs to the exterior wall component included ambient outside temperature, windspeed, incident solar flux on the exterior, and interior temperature. The inputs to the interior wall are the temperatures on each side. Verification of the interior and exterior PCM wall models was carried out by comparing their transient heat-up behavior predictions with those of another PCM code which has been previously verified.⁷ Equivalent boundary conditions were established by setting the convective heat transfer coefficient either very high (to simulate conduction) or very low (to simulate an adiabatic wall). In comparison runs using typical PCM property data, the agreement in surface temperature predictions from the two codes was excellent.

2.2.2 Solar Ray Tracing Subroutine Validation

The sun-tracking subroutine was tested using a 1 ft² window which was placed in a variety of positions in a small one-room simulation. Flux data produced were examined to determine consistency with what would be qualitatively expected for given times of the day.

The subroutine gave consistent values and was accepted as being more accurate than using view factor calculations for apportioning beam radiation in a room.

2.2.3 Simulation of Building with PCM Wallboard

A simple structure was selected to determine the space heating energy savings that accrue with the PCM wallboard. The structure modelled with TRNSYS was similar to one studied by Neeper.⁸ In Neeper's study, the entire structure was modelled as one node with a total load coefficient (TLC) of 14,100 Btu/°F-d. In comparison, TRNSYS modelled the structure by treating the floor, ceiling, walls, and windows as separate nodes. The backup heating system model for the building was a forced air furnace with thermostat control. The following lists the characteristics of the building modelled:

dimensions of structure	=	50 ft x 36 ft x 8 ft
floor area	=	1800 ft ²
total window area	=	360 ft ²
air infiltration rate	=	½ air change per hour
wall insulation	=	R-18
ceiling insulation	=	R-30
wallboard to floor ratio	=	3:1
windows	=	doubled glazed
heater set point	=	65° F
maximum room temp.	=	75° F

The floor did not contain any PCM and, therefore, was modelled by a transfer function partition as provided in TRNSYS. The floor chosen corresponded to a 3-in. wood floor with an overall heat transfer coefficient, $U = 0.107 \text{ Btu/h}\cdot\text{ft}^2\cdot^\circ\text{F}$ (R-9). The walls were specified with $U = 0.056 \text{ Btu/h}\cdot\text{ft}^2\cdot^\circ\text{F}$ (R-18) to match Neeper's structure. In the case of the PCM wallboard, experiments were conducted on plasterboard wallboard samples made by U.S. Gypsum and impregnated with PCM. From these experiments, key thermophysical properties were determined as shown in Table 1.

Table 1. Wallboard Thermal Characteristics. C_p = specific heat capacity, k = thermal conductivity, LH = latent heat, T_m = PCM melt temperature

Wallboard (1/2-in.) (lb/ft ³)	Density (lb/ft ³)	C_p (Btu/lb·°F)	k (Btu/h·ft·°F)	LH (Btu/lb _{wallboard}) (°F)	T_m
Standard	43.5	0.26	0.10	0	—
30% PCM*	62.4	0.35	0.134	25	68
20% PCM	50	0.32	0.118	16.7	68
16% PCM	47.5	0.31	0.111	13.3	68
10% PCM	45	0.29	0.108	8.3	68

*The 30% PCM information was obtained using U.S. Gypsum wallboard which had a slightly higher initial density than National Gypsum wallboard.

The ceiling was modelled with $U = 0.033$ Btu/h·ft²·°F (R-30) and the wallboard information in Table 1. In the Neeper analysis, a 3:1 wallboard-to-floor ratio was chosen. In an effort to maintain the 3:1 ratio for the TRNSYS analysis, additional PCM was added to the ceiling. With these changes, the total heating load coefficient for the building was 15096 Btu/°F·d which was only slightly less well-insulated than Neeper's.

A series of TRNSYS runs were made using hourly weather data for a typical winter in Denver. A passive solar dwelling (the "solar house") was simulated by having 200 ft² of south-facing glazing and 160 ft² of glazing on the north wall. To simulate a dwelling with a smaller solar component (the "non-solar" house), all 360 ft² of glazing was located on the north facing wall. Double-pane glazing was used throughout. The supplementary heating system simulated for the building was a forced air unit sized at 37,600 Btu/h with a mass flow rate of 500 ft³/min. The thermostat control called for heating if the room temperature fell below 65°F; the thermostat turned off the heating system when the room temperature reached 70°F. The room was vented with outside air if the interior temperature rose above 75°F. Under these operating conditions,

a series of simulations on the non-solar and solar building were conducted to determine the energy savings due to various concentrations of PCM in the wallboard. The results are shown in Table 2.

Table 2. Total energy use summary

PCM Content (%)	Latent Heat Capacity of wallboard (Btu/ft ²)	Heating energy used (mBtu)	
		Non-solar house	Solar house
0	0	73.7	59.7
10	14	70.6	49.0
16	26	70.1	43.5
20	35	70.0	41.0
30	65	69.9	38.2

Several trends are evident from Table 2. First, it is clear that irrespective of the PCM wallboard, there is a significant energy savings simply due to window placement. As the solar component of the building increases, the supplemental heat requirements of the building are reduced by about 19%. It is also apparent that the introduction of PCM into a non-solar building does not appreciably reduce the supplemental energy requirements of the building. This is as expected. However, in the case of the solar building, the PCM wallboard is very effective. Even at low PCM concentrations (10%), the presence of the PCM reduces the heating requirements by 18%. As the PCM concentration increases, the energy savings in absolute terms increases. The 30% PCM level represents the highest PCM concentration obtained through laboratory experiments using the immersion process.

2.2.4 Economic Analysis

An economic analysis of the PCM wallboard was performed for the solar house to determine the economic benefit of the latent heat storage system and to determine how estimates of the cost of the PCM system affect this benefit. This analysis was based on the value of the heating energy savings from Table 2 and that these energy savings would be constant from year to year for the lifetime of the PCM wallboard system. From the annual energy savings, annual fuel cost savings were determined based on the price of displaced fuel, either natural gas, home heating oil, or electricity. The present value of the stream of energy savings was determined using standard engineering economic analysis procedures. The present value of energy savings (PVES) represents the maximum allowable installed cost of the PCM wallboard system. A discount rate of 6.7% was used in this analysis.

Three supplemental heating systems were considered and average energy costs were determined as shown in Table 3.

Table 3. Supplemental heating system data

Heating system	Fuel cost ^(A)	Efficiency	Adjusted fuel cost ^(B)	e ^(C)
Gas furnace	\$4.96/mBtu	0.80	\$6.20/mBtu	3.0%
Oil furnace	\$5.70/mBtu	0.80	\$7.13/mBtu	3.0%
Heat pump	7.50¢/kWh	SPF = 2.0	\$10.98/mBtu	3.8%

^(A)Average prices of fuel for residential sector during 1988 as taken from the *Monthly Energy Review*, DOE/EIA-0035(88/12), December 1988.

^(B)Fuel costs adjusted for system efficiencies shown.

^(C)Fuel escalation rates estimated for a nominal base case provided by the *EIA Short-Term Energy Outlook*, DOE/EIA-0202(89/3Q), July 1989. Escalation rates for outyears were projected to remain unchanged from the DOE short-term estimates.

From the discount rate, fuel costs and anticipated escalation rates, uniform present worth factors were determined and used to obtain the present worth of the energy saved for periods up to 30 years for the solar building as shown in Table 4. This table was useful not only to evaluate the PVES for the lifetime of the system but also to determine the discounted payback for the PCM wallboard. For example, a PCM wallboard system with latent heat capacity of 26 Btu/ft² and a lifetime of 20 years has a present value of \$2673 if the building is heated by an electric heat pump. To provide a three-year payback, that same PCM wallboard system must have an installed cost no greater than \$502. The areal latent heat storage capacities (14, 26, 35 and 65 Btu/ft²) shown in Table 4 are representative of the latent heat content of samples of gypsum wallboard that have been impregnated with the paraffin wax PCM. Experiments underway to study full-scale samples of the PCM wallboard have shown that a latent heat capacity 35 Btu/ft² is obtained after soaking ordinary ½-inch gypsum wallboard in a bath of melted wax for less than five minutes resulting in a PCM wallboard weight increase of 30 percent. Areal latent heat storage capacities less than this value have been demonstrated by shortening the soak time.

Table 4. PVES (\$) of PCM addition to walls of 1800 ft² home in Denver; 200 ft² of S. glazing; no window insulation

Wallboard latent heat = 14 Btu/ft²

N(years)	Natural gas	Electricity	Fuel oil
1	63	113	73
2	125	224	144
3	184	331	212
4	241	436	278
5	297	538	341
10	545	1005	627
15	753	1412	865
20	926	1765	1065
30	1192	2338	1371

Wallboard latent heat = 26 Btu/ft²

1	96	172	111
2	189	339	218
3	279	502	321
4	366	661	421
5	449	815	517
10	826	1523	950
15	1140	2138	1311
20	1403	2673	1613
30	1806	3541	2077

Wallboard latent heat = 35 Btu/ft²

1	111	199	128
2	219	393	252
3	323	582	372
4	424	765	487
5	520	943	599
10	956	1763	1099
15	1320	2476	1518
20	1624	3095	1868
30	2091	4100	2405

Wallboard latent heat = 65 Btu/ft²

1	128	229	147
2	252	452	290
3	371	668	427
4	487	879	560
5	598	1084	688
10	1098	2026	1263
15	1516	2844	1744
20	1866	3556	2146
30	2402	4710	2763

As a first case, electricity was assumed as the backup fuel and selected data from Table 4 were plotted as shown as the curves in Fig. 10. For simplicity, the PVES was normalized with respect to wallboard area to determine the "allowable cost" for the PCM system. It should be noted that since the baseline storage system was conventional gypsum wallboard with no PCM, the costs shown in Fig. 10 represent the maximum allowable cost of the PCM itself including the cost of incorporating the PCM into the wallboard. Clearly for an economic winner, the cost of the PCM installed in the wallboard must be less than the allowable.

2.2.5 PCM Wallboard Cost

The cost of PCM wallboard depends on the amount (weight) of PCM, the unit cost of PCM, and the cost required to incorporate the PCM into the gypsum board. It was assumed that installation costs of PCM wallboard and conventional wallboard into a building would be equal since the same building trades (drywall hangers and finishers) would be needed in either case. Therefore, there would be no cost penalty associated with installation of the PCM wallboard. Based on measured physical data on the paraffin PCM and plasterboard and the area of 1/2-in. PCM wallboard needed, the weight and latent heat capacity of the PCM wallboard was determined as shown in Table 5.

Table 5. PCM wallboard characteristics for 5040 ft² of 1/2-in. plasterboard. PCM latent storage capacity measured to be 83 Btu/lb.

Total wallboard weight (lb)	%PCM	PCM weight (lb)	Areal heat capacity (Btu/ft ²)
13105	30	3932	65
10500	20	2100	35
9975	16	1600	26
9450	14	945	14

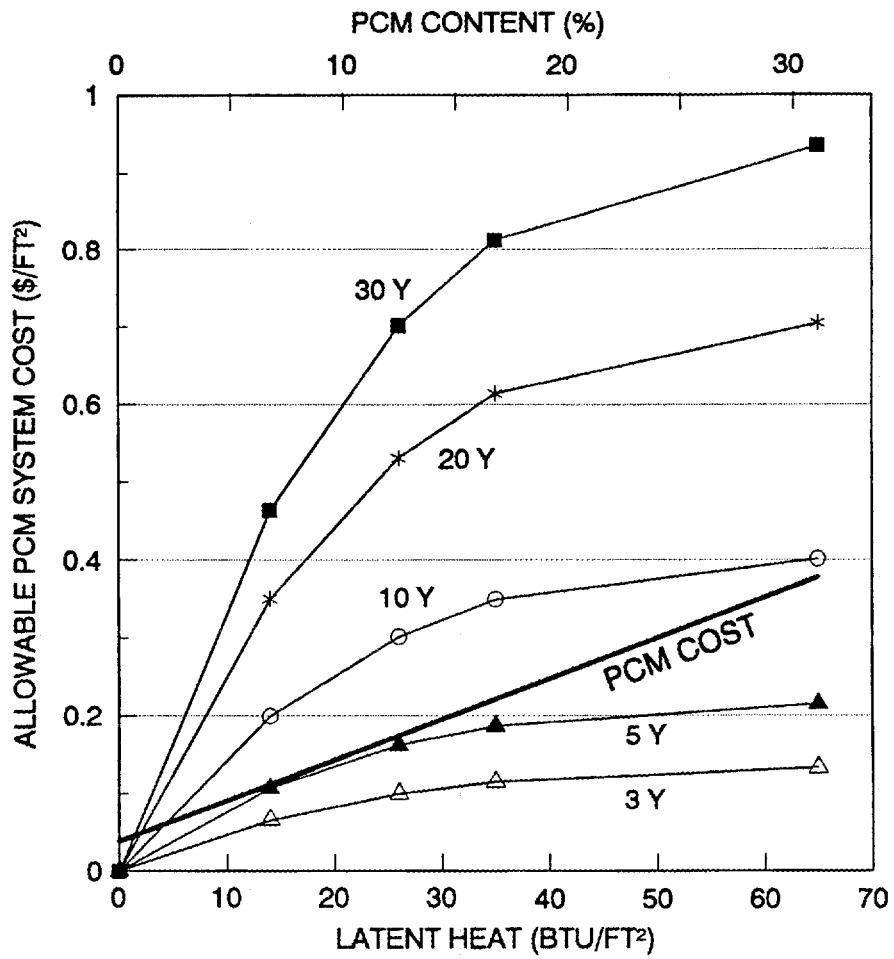


Fig. 10. PCM system allowable cost with electricity backup as function of period and latent heat capacity

The PCM wallboard cost was separated into two components: one that indicates costs attributable to the PCM, and the second, a term that collects all other costs such as manufacturing costs (incorporation of the PCM into the wallboard), overhead, and profit. Thus the following terms were defined:

h_m = the latent heat of the PCM (Btu/lb)

H = the areal latent heat of the PCM wallboard (Btu/ft²_{wallboard})

C_{PCM} = the unit cost of the PCM (\$/lb)

C_{other} = other costs associated with incorporation of the PCM into drywall (\$/ft²_{wallboard})

C_{total} = the total cost of the PCM wallboard

Therefore, the total cost of the PCM wallboard can be written as

$$C_{total} = [(C_{PCM})/(h_m)]H + C_{other} \quad (1)$$

This is the equation of a straight line of slope $(C_{PCM})/(h_m)$ and intercept C_{other} . This cost function can be superimposed on Fig. 10 to determine the payback and optimal PCM content in the wallboard.

As an example of this technique for estimating the economic attractiveness of the PCM wallboard, data from ongoing PCM wallboard experiments at ORNL were used. The paraffin wax obtained for wallboard experiments (a mixture of C-18 and near neighbor carbon atoms) was developed by Witco Chemical and sold for \$0.50/lb in barrels. The phase change temperature was taken to be 72°F and was determined by the average of the melting and freezing temperatures as measured by differential scanning calorimetry. The latent heat was measured to be 83 Btu/lb. These data were substituted into Eq. 1 and the resulting straight line equation superimposed on the allowable cost curves as shown in Fig. 10. For this example, it was assumed that $C_{other} = \$0.03/\text{ft}^2$. This PCM cost function intersects all allowable cost curves above $N = 5$ years and does not intersect any cost curve below $N = 5$ years. In other words, the allowable cost curve that is tangent to the PCM cost function defines the earliest time at which the PCM system cost equal the allowable cost. Therefore, the discounted payback period under the assumptions given is approximately 5 years. Note also from Fig. 10 that (1) the installed

PCM wallboard cost will be \$.12/ft², (2) the optimal latent heat content of the wallboard will be approximately 15 Btu/ft², and (3) if the lifetime of the PCM wallboard system were 30 years, the present worth of the PCM system would be \$0.48/ft². If C_{other} is larger than \$0.03/ft², a 5-year payback requires identification of a PCM that is either lower in cost or has a higher latent heat capacity so that the PCM cost is sufficiently reduced so as to keep the cost function line tangent to the $N = 5$ line. It is also apparent that for $N = 5$ years, C_{other} cannot be much above \$0.20/ft² regardless of the price of the PCM.

In summary, this study indicated that through incorporation of PCM wallboard, winter heating loads can be reduced for locations where the average insolation is high. It was found that the heating energy savings must be analyzed to determine the best balance of PCM content and investment payback period. Little benefit in placing PCM wallboard in a non-solar house was found. Work is underway to determine whether the PCM wallboard improves thermal comfort inside the building as an additional benefit.

2.3 PCM WALLBOARD DEVELOPMENT

Experimental efforts were continued to incorporate PCMs into conventional building materials to enhance their energy storage capacity. Although the building material of current interest is gypsum wallboard, other materials including concrete masonry units may warrant future study. In any case, the objective is to retain the PCM in the structure of the building material itself to keep the cost associated with containment of the PCM at a minimum. Prior work at the University of Dayton Research Institute has shown that linear alkyl hydrocarbons with a single freezing and melting point and low vapor pressure are attractive PCMs for incorporation into building materials.⁹

For a practical system, there are several issues to be addressed including, (1) the ability of the wallboard to immobilize the PCM so that leakage does not occur, (2) issues connected with fire safety of the PCM wallboard, and (3) methods of PCM containment. Results from thermocycling tests of wallboard that had been simply immersed in liquid PCM have been reported earlier.² Through these initial tests as well as high temperature aging tests on PCM wallboard, little was found to affect the stability of the PCM in plasterboard. Initial PCM frosting

on the surface of the wallboard could be suppressed with a suitable paint. Work during the current reporting period focused on the latter two issues.

2.3.1 Progress with Fire Safety

The PCM best suited to the concept from a technical standpoint is a mixture of alkyl hydrocarbons (paraffins). However, these materials alone are flammable. Therefore, work was conducted on evaluating the effects of fire retardants on and inside of the PCM wallboard. One of the more promising methods for fire retardation of the PCM wallboard is to imbibe the PCM boards in an insoluble fire retardant so that the fire retardant will be on the surface and prevent ignition of the paper and the paraffin. Laboratory experiments with the plasterboards imbibed with K-61 (a paraffin blend produced by Witco Chemical) up to 20% by weight and later imbibed in Fyrol CEF (beta - chloroethyl phosphate insoluble in the K-61) proved to be self-extinguishing in horizontal flame tests. For confirmation in a larger scale, 2 ft x 2 ft specimens of 1/2- and 5/8-in. thick plasterboard were sent to the National Gypsum Company for later testing in a Steiner tunnel according to ASTM E84-81.

To determine the impact of fire retardant on PCM wallboard thermal performance, several 6 in. x 6 in. samples 1/2- and 5/8-in. thick were prepared, sequentially imbibed with PCM and Fyrol CEF and subjected to differential scanning calorimetry (DSC). The data showed that the latent heat storage capacity was reduced less than what would be expected from the concentration of fire retardant in the sample. It was concluded that the insoluble Fyrol CEF does not suffuse through the plasterboard and replace the PCM as might be expected. The Fyrol was apparently more concentrated at the paper surface of the wallboard rather than on the wallboard interior. To increase this protective surface layer, a sequential immersion of wallboard first into the liquid PCM and then into the CEF fire retardant was conducted. Tests on these samples showed that a 1/2-in. board containing 30% PCM and CEF was flammable. Once ignited, burning continued for over 3 minutes. The 5/8-in. 20% PCM control sample without CEF did ignite but did not burn long. Follow-on experiments with 1/2-in. wallboard containing 20% PCM and 5/8-in. wallboard with 16% PCM are in progress.

Fire retardant paints were also tested to determine their effectiveness at reducing the rate of flame spread. Several samples of 20% and 30% K-61 paraffin were coated with fire retardant paints (Firebrew T, Firebrew FX-3, Pyromark 1500, and Pyromark 1506) and subjected to horizontal flame tests. Results of these tests showed that none of the samples were self-extinguishing, although the samples were more difficult to ignite and burned with a smaller flame than a control sample. Further work is underway.

2.3.2 Alternative Methods for PCM Incorporation

It has been reported² that simple immersion of plasterboard into melted paraffin is the simplest process for incorporating a PCM into manufactured wallboard. However, an alternative process must be found if the PCM is to be added during wallboard manufacture. The University of Dayton found that a free flowing powder is produced when the paraffin PCM is combined with small particle size silica. This powder contains up to 75 wt. % of PCM. It was found from experiments performed by the National Gypsum Company that hydrophilic silica (Cab-O-Sil MS-7) would phase separate in the wet mix of plaster and release the hydrophobic paraffin PCM. It was apparent that hydrophobic silicas should not absorb water and should better retain the PCM.

To test this hypothesis, mixtures of 20% and 30% PCM contained in a matrix of three silicas were chosen for experimental study. One silica was hydrophilic, and the other two were hydrophobic. Batches of three cubes from each silica/PCM mix and controls were made and used to study water absorption, compressive strength, and latent heat storage capacity as measured by DSC. Water pickup was determined with one cube of each kind. It was found that weight gain in the case of hydrophilic silica is about twice that of the hydrophobic silica. The samples with PCM picked up less water and lost less weight on drying.

After drying, all samples were subjected to compression testing and were found to have compressive strengths equal to or better than the control samples containing water and silica.

Finally, DSC analyses were performed and showed that in the case of hydrophilic silica, the PCM melting characteristics were unaffected. Some minor discontinuities during PCM crystallization were noted but were not deemed significant for the wallboard application.

Based on work done in the reporting period, the following conclusions were drawn:

1. Hydrophobic silica/PCM can be added to the wet mix during plasterboard manufacture without encountering phase separation.
2. Water uptake was reduced only slightly by addition of the hydrophobic silica/PCM powder into the wet mix.
3. At a nominal concentration of 20 and 30 wt. % of hydrophobic silica/PCM, the compressive strength of the cured plaster product was equivalent to that of the control sample with no additives.
4. If the overall raw material and process economics prove favorable, the hydrophobic silica/PCM system has strong potential as a means of introducing paraffin PCM into plasterboard during manufacture.

2.4 EFFECT OF DOPANTS ON SOLID-STATE PCMs

The overall objective of this project was to understand the phase transition mechanisms in organic thermal energy storage materials in which the heat is reversibly absorbed during the solid-solid phase transitions. Organic polyalcohols undergo crystallographic changes absorbing or releasing large amounts of latent heat at constant transition temperature well below their melting points. There are known pure polyalcohols which undergo solid-solid phase transitions storing latent heat; however, they have high transition temperatures. Lowering the transition temperature is important for development of practical TES materials. Binary polyalcohol compounds were studied to adjust transitions to near room temperature. In this project, the effect of the crystallographic changes of several polyalcohol crystals with the addition of a second component or dopant was determined.

Organic molecular polyalcohol crystals such as pentaerythritol (PE), pentaglycerine (PG), neopentylglycol (NPG), and an 2-amino 2-methyl 1,3 propanediol (AMPL) were investigated in this reporting period. The phase behavior was determined for AMPL-NPG system to determine the low temperature transitions for thermal energy storage. Pure AMPL and NPG both have monoclinic low temperature crystal structures. The high temperature structure of pure AMPL was determined in this study as body-centered cubic which exists at a much lower temperature than that of the face-centered cubic γ phase of pure NPG. The key features of this eutectoidal phase

behavior include: $\alpha + \beta \rightarrow \gamma$ transitions at 20° C, $\alpha + \gamma \rightarrow \gamma'$ at 50° C, and finally the eutectic $\gamma + \gamma' \rightarrow$ liquid at -92° C where α and γ' are low and high temperature AMPL-rich phases, respectively. The β and γ are analogous high and low temperature for NPG phases. It was found that two high temperature (γ and γ') phases co-exist in equilibrium in a narrow composition range. It was also found that thermal energy was absorbed continuously in the $\alpha + \gamma$ and $\alpha + \gamma'$ regions which led to the identification of continuous phase change materials (CO-PCMs). In these CO-PCMs the enthalpies of continuous phase transformations as well as the sensible heat are absorbed over a temperature range between two phase boundaries.

The crystallographic changes during heating of these polyalcohols affect the containment vessel design, and therefore lattice expansion/contraction measurements were performed. In the AMPL-25 mol% NPG binary system, thermal contractions with abrupt decreases of 28% were observed in γ and γ' phases during heating. It was also found that the AMPL-rich binaries may be supercooled, and the high temperature phase can be triggered by straining the material to release an estimated 50-53 cal/g of heat at room temperature, provided nucleating agents are not added.

The PE and NPG which have hydrogen-bonded lattices with layered- and chain-type low temperature structures, respectively, are known TES materials. However the phase diagram and the transition mechanisms were not known. In this project the phase behavior of mixtures of PE and up to 30 mol% NPG was determined using X-ray methods. This phase diagram has also been generated using a computer program, and results are in good agreement with the experimental data. The thermodynamic properties such as free energies for the solid-solid transitions and for excess free energy for the binaries were determined for this PE-NPG system. The PE-NPG binaries exhibited complex behavior with more than one solid-solid phase transition. The NPG-rich β transformed to γ at a constant temperature, but the transition of the PE-rich α to γ' phase passed through a two-phase field at a temperature that varied as a function of composition. The DSC traces of the PE-rich binaries showed two normal endotherms and an anomalous continuous broad exotherm during heating. An explanation for this is under study. The DSC traces of the NPG rich binaries showed two normal endotherms and another continuous broad endotherm for the $\alpha \rightarrow \gamma$ transition in the two phase region during heating. Again, further work to explain this behavior is in process.

The transition temperatures of the PG were reduced by the addition of and trimethylol propane (TMP) and AMPL. For the PG-TMP system a 84°C solid-solid transition was recorded for the binaries up to 40 mol% TMP. With the PG-AMPL system, there were continuous decreases in the transition temperature with increasing additions of AMPL. The phase behavior for these two systems is not clear at this time. Research is being continued on these systems to develop a description of the phase behavior and construction of the phase diagrams.

2.5 DIRECT CONTACT ICE STORAGE SYSTEM DEVELOPMENT

Conventional ice storage systems are based on freezing ice on evaporator surfaces or heat exchanger tubing. The advantages of direct contact heat exchange in ice making are threefold: (1) an improved operating efficiency due to low approach temperatures, (2) elimination of the need for defrosting, and (3) a high potential for reducing first cost by elimination of surface evaporators. Based on these advantages, the development of a direct contact ice maker has been continued. In this system, liquid refrigerant sparges against a stream of water. As the refrigerant vaporizes, the water freezes into ice and falls into a tank for storage.

The original direct contact ice storage system design by CBI Industries was based on R-114. Although this refrigerant possesses almost ideal pressure/temperature saturation properties and does not form a clathrate with water, it is one of four common refrigerants which reacts with atmospheric ozone. As a result, its production will be curtailed. A search was initiated for replacement candidates that (1) would not form a clathrate, (2) would not appreciably hydrolyze with water, (3) are essentially insoluble in water, and (4) would meet basic safety and environmental requirements. To address the first of these constraints, a literature search was conducted to determine those refrigerant properties conducive to the formation of clathrates and to examine R-124 as a replacement refrigerant for the direct contact process. This refrigerant was attractive since its vapor pressure characteristics are similar to those of R-114.

According to theory,¹⁰ the upper limit for the molar volume of the liquid refrigerant component of a clathrate is 85 cm³. Using available R-124 liquid density data, the molar volume was calculated to be 95.1 cm³. Table 6 summarizes the data on molar volume and known clathrate formation characteristics for R-124 and several other refrigerants.

The results indicate that the theoretical molar volume limit did not uniquely determine clathrate formation.

Table 6. Refrigerant molar volumes at 32° F

Refrigerant	Molar Volume (cm ³)	Forms clathrate?
R-22	67.5	yes, easily
R-12	86.6	yes, with difficulty
R-11	89.5	yes, with difficulty
R-124	95.1	?
R-114	113.5	no

To determine the propensity for clathrate formation, a small test facility was assembled. The facility consisted of a sealed cylinder containing water and refrigerant; the cylinder was immersed in a constant temperature bath. Pressures and temperatures inside the cylinder were measured and plotted to determine deviations from saturated refrigerant conditions that could indicate the presence of a clathrate. As a first test in the facility, a mixture of R-12 and water was studied to verify that a clathrate could be identified. The resulting pressure/temperature data clearly indicated the presence of a clathrate. The fact that the experimental data are in agreement with published data proved that the sealed tube test apparatus could be used to detect the presence of clathrates.

Following tests of R-12 and water, the facility was used to examine R-124. Results of these tests were inconclusive. During some tests, a crystalline substance was formed which dissociated slowly; at other times, no solids were formed. Additional tests with R-124 were conducted in a small (2½-ton) direct contact ice making facility shown in Fig. 11. Operation of the 2½-ton system proved that R-124 did indeed form a clathrate as noted by continued migration of refrigerant from the receiver during the charging process and through pressure measurements taken in the storage tank following the charge test. A light brown, foamy compound

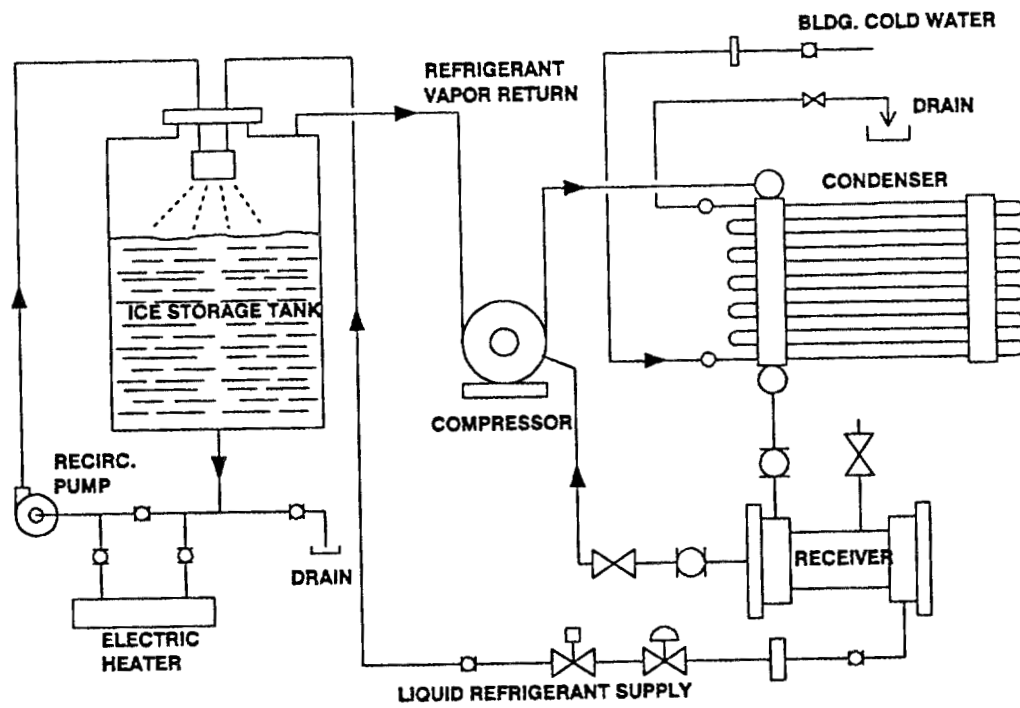


Fig. 11. Direct contact ice system schematic (2½-ton capacity).

was also observed on the free liquid surface in the storage tank. At intervals during the tests, samples of water saturated with R-124 were taken and placed into steel and plastic containers to determine corrosion tendencies. These tests showed that R-124 is compatible with PVC piping and fittings, thread sealants, valve gaskets, and polycarbonate but is incompatible with plexiglas on a long-term basis.

Work is being continued to determine the quantity of refrigerant trapped in the clathrate and to determine the minimum amount of refrigerant necessary to maintain the clathrate structure.

2.6 DEVELOPMENT OF SEPARATION TECHNIQUES FOR A DIRECT CONTACT TES SYSTEM

In direct contact ice-making processes, the refrigerant will pick up both water vapor via direct percolation and oil from the compressor. The purpose of this project is to investigate methods for separating water vapor and oil from a refrigerant in a closed refrigeration cycle. Three possible devices for separating oil and water vapor from the cycle refrigerant were considered: a membrane system, mechanical separation, and a Ranque-Hilsch vortex tube.

2.6.1 Membrane Evaluation

The Membrane Products Division of the DuPont Company provided information on the characteristics of Nafion perfluorinated membranes. The water vapor diffusion coefficient for a 7-mil thick Nafion membrane was determined to be $D_v = 5 \times 10^{-5}$. Based on this coefficient, it was estimated that a membrane area of $1.4 \times 10^3 \text{ m}^2$ ($1.5 \times 10^4 \text{ ft}^2$) would be needed to separate refrigerant that is initially saturated with water in a direct contact system producing 1 ton of refrigeration. Based on the cost and complexity of this system, it was concluded that a membrane system would be impractical.

2.6.2 Mechanical Separator Evaluation

The characteristics of a mechanical separator normally used for separating a water mist from air were evaluated, and it was determined that a ½-in. cyclonic separator would be needed

to remove 99% of the mist greater than 3 microns in size. Since much of the moisture will be in the vapor state rather than a mist, there remain questions concerning mechanical separation as an effective tool for the direct contact process. Further studies were indicated.

2.6.3 Ranque - Hilsch Vortex Tube

Removal of the moisture from the mixture by condensation was considered as a potential process for separating the components. Accordingly, a vortex tube was considered. In this device, water vapor would condense in the cold stream exiting one side of the tube. It was assumed that the direct contact ice making process would use a high pressure refrigerant so that the vortex tube could be operated effectively with a large pressure drop and, properly designed and staged, would perform the task required. Interestingly, although the vortex tube invented 55 years ago is a commercial reality, it is reported¹¹ that no analysis has been completed to explain the details of gas motion in a vortex cooler. Although this analysis was beyond the scope of the direct contact project, an experiment was designed to establish the feasibility of using the vortex tube for the task at hand.

A conceptual design of a bench-scale experiment to study the separation effectiveness was developed in which refrigerant will be percolated through water and passed through a small vortex tube. The temperature and mass flow rate of the cold stream, hot stream, and incoming stream will be measured along with the rate of change in mass of the percolator. After an initial test with pure refrigerant, water vapor will be introduced to determine its effect on the temperatures of the cold and hot streams and to determine water vapor condensation rates. Detailed design of the facility is underway.

3. TECHNICAL PROGRAM - INDUSTRIAL TES

3.1 DEVELOP/TESTING OF TES MEDIA FOR HIGH TEMPERATURE INDUSTRIAL APPLICATIONS

Over a period of several years, the TES program has continued the development of an advanced high temperature TES material for industrial applications. The initial purpose of the material is to capture heat from flue gases in periodic industrial processes, store the energy as sensible and latent heat in a packed bed of the material, and release the heat at a later time back into the industrial process as needed. Therefore, the material provides a compact medium for regeneration of heat by industry. The unique storage material is a ceramic containing a PCM in its microstructure. As the material is carried above the melting point of the PCM, latent heat is stored as the PCM melts in addition to the sensible heat stored in the ceramic matrix and PCM. The large surface area of the ceramic microstructure effectively retains the liquified PCM so that a "form-stable" material with a high effective heat capacity around the PCM melting point is produced. In prior years, the material, a composite PCM or CPCM, was carried through laboratory development. However, the performance of this material when used in a large packed bed storage system with flue gas and air as working fluids was not determined. Further, the thermodynamic performance of a packed bed containing this material had not been verified. A project is currently underway at MSU to design, construct, install and operate a packed bed TES system to study the metallurgical performance of the CPCM and to verify and validate a thermodynamic model of the packed bed system. The purpose of the model is to facilitate optimal designs of a full-scale packed bed system.

In the prior reporting period,² MSU completed enhancements to their packed bed model to allow study of a packed bed system with layers of different CPCMs, to allow consideration of the thermal effects of the walls of the packed bed, and to consider temperature-dependent properties of the working fluids. The work performed during the current reporting period consisted of the development of a test plan and preliminary design of the packed bed test facility. The model was used in preparing this design. The facility first proposed consisted of a cylindrical packed bed with a test section measuring 1 ft (305 mm) by 1 ft (305 mm) and associated equipment as shown in Fig. 12. Three CPCM pellet sizes were proposed, each with an aspect ratio of unity, and sized ½-in. (12.7 mm), ¾-in. (19 mm), and 1-in. (25.4 mm) dia. These

dimensions were selected based on pressure considerations which imposed a limit for pressure drop across the bed if an induced draft fan is used as shown in Fig. 12. A review of this design indicated that the validity of bed temperature and flow measurements for determining the thermal performance of the bed would be enhanced with a larger bed. This would also reduce the impact of "wall effects" caused by large void fractions near the wall and heat transfer between the wall and the storage media. Therefore, the bed design size was increased to 2 ft (6.10 mm) to ensure a small wall effect when the 1-in. (25.4 mm) dia. pellets are used.

A test plan was defined to accomplish model validation and to measure pellet performance. Measurement of the following variables will be conducted:

1. Inside and surface temperatures of the pellets as functions of axial location in the bed and time.
2. Working fluid temperatures as functions of axial location and time during charging and discharging. These measurements will be supplemented by fluid temperature measurements in off-center locations in the bed to provide an indication of flow uniformity across the bed.
3. Containment vessel wall temperatures on the inside and outside surfaces of the container as functions of axial location and time.
4. The duration of both charging and discharging processes.
5. Fluid mass flow rates.
6. Pressure drops through the packed bed.

In the near term, the final design will be completed and submitted to an experienced fabricator for construction of the facility.

3.2 DEVELOPMENT OF DIRECT CONTACT MOLTEN SALT/AIR HEAT EXCHANGER

There is interest in developing direct contact as an efficient heat exchange process not only for building cooling but for solar thermal and possible industrial applications as well. In prior years, the SERI performed experiments with a direct contact heat exchanger to determine heat transfer rates and pressure drops in a column packed with Pall rings through which molten salt

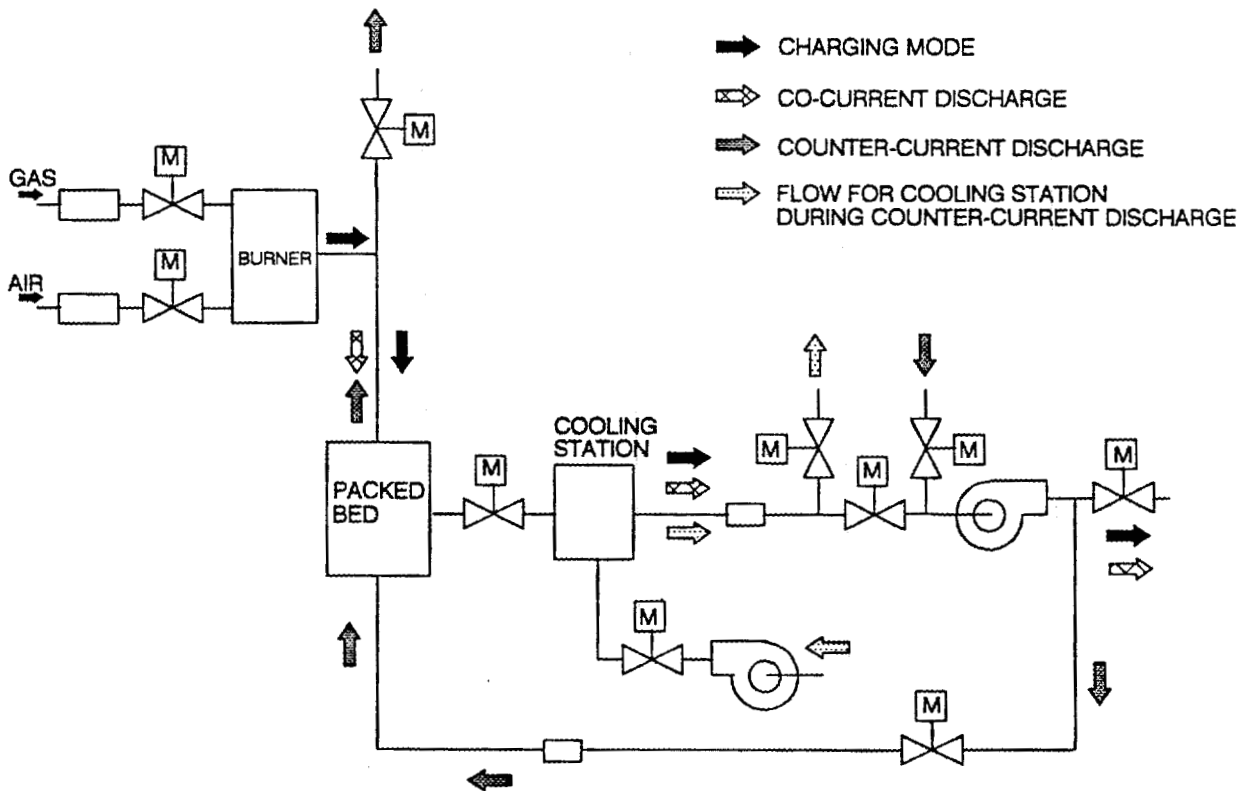


Fig. 12. Schematic of proposed high temperature TES test facility.

and air are passed in opposite directions.¹² This early effort produced heat transfer correlations and models which were experimentally validated over a limited temperature range. During the current reporting period, tests were conducted in the direct contact test facility to determine the influence of radiation as a principal method of heat exchange within the bed. To accomplish this goal, tests were conducted in a facility consisting of a vertical packed column with a downflow of molten salt and upflowing air. Heat exchange between the salt and air was determined by measuring changes in enthalpy between inlet and exit conditions for the salt and air. Pressure taps in the column were used to determine differential pressures during testing.

The test series involved 61 simultaneous measurements of heat transfer and column differential pressure at salt inlet temperatures ranging from 320°C to 520°C, salt flow rates ranging from approximately 6 to 18 kg/m²-s, and an air flow rate of 0.3 to 1.2 kg/m²-s. The results from these tests indicated that pressure drop correlations by Berner and Kalis¹³ or Stichlmair¹⁴ are adequate to predict pressure drops in the molten salt direct contact system. In addition, the heat transfer correlation earlier developed by Bohn¹² is accurate over the wider set of test conditions reported. The data from the current tests, which were conducted at widely-spaced temperature levels, showed conclusively that radiation heat transfer does not play a significant role in overall column heat transfer. This validated an assumption used in the heat transfer correlation developed earlier.

4. CONCLUSIONS

The diurnal and industrial TES program has made significant progress in the development and application of TES. Coordinated research was performed aimed at four large applications: (1) the development of building materials with enhanced heat capacity, (2) the development of a low temperature chill TES system for refrigeration applications, (3) development of an advanced ice storage system for commercial building cooling, and (4) development of a compact and effective high temperature regenerator technology. In each case, the research performed supports ultimate commercialization of a TES technology. Emphasis placed on determining the worth of the PCM wallboard found that in a passive solar application, the concept is economic with a payback of 3 - 5 y. This determination is accurate since it was based on actual experience with the PCM wallboard thermal performance and costs of the PCM. In the case of the low temperature chill storage system, the research during the reporting period provided data which confirmed the choice of the dry bed heat exchanger as the preferred heat and mass transfer system. Progress with development of the direct contact ice storage system was slowed due to the finding that R-124, the leading contender as a replacement for R-114, forms a clathrate hydrate. Further work to determine an alternative refrigerant or a method of accommodating the clathrate is indicated.

In the industrial TES component of the program, progress was made toward a field test of the high temperature composite PCM. The packed bed thermodynamic code developed by MSU was used to support a preliminary design of a test facility. This design is sufficient to validate the model and, moreover, will fulfill the objectives set for testing the composite under actual flue gas conditions within the tight budget constraints for the coming year.

REFERENCES

1. J. J. Tomlinson and M. J. Taylor, *Thermal Energy Storage Technical Progress Report April 1986-March 1987*, ORNL/TM-10715, Martin Marietta Energy Systems, Inc., Oak Ridge National Laboratory, February 1988.
2. J. J. Tomlinson and R. J. Keadl, *Thermal Energy Storage Technical Progress Report April 1988-March 1989*, ORNL/TM-11492, Martin Marietta Energy Systems, Inc., Oak Ridge National Laboratory, March 1990.
3. N. J. Freundlich, "Wallboard Undergoes a (Phase) Change," *Solar Age*, 50-51, August 1988.
4. J. F. Martin, *Thermal Energy Storage Technical Progress Report April 1984-March 1985*, ORNL/TM-9819, Martin Marietta Energy Systems, Inc., Oak Ridge National Laboratory, January 1986.
5. S. A. Klein et al., TRNSYS - A Transient System Simulation Program, Solar Energy Laboratory, University of Wisconsin, December 1983.
6. D. J. Balcomb et al., "Natural Air Motion and Stratification in Passive Buildings," *Proceedings of the Passive and Hybrid Solar Energy Update, September 5-7, 1984*, CONF-8409118, Washington, D.C., October 1984.
7. A. D. Solomon, "Mathematical Description of Distributed PCMs," *Thermal Energy Storage Program, Management Report, March-April 1989*, Oak Ridge National Laboratory, Oak Ridge, TN.
8. D. A. Neeper, "Potential Benefits of Distributed PCM Thermal Storage," *14th National Passive Solar Conference*, Denver, CO, LA-UR-89-1059, June 19-23, 1989.
9. I. O. Saylor, A. K. Sircar, and S. Dantiki, "Advanced Phase Change Materials and Systems for Solar Passive Heating and Cooling of Residential Buildings," *Final Technical Report to the U.S. Department of Energy, May 29, 1986 through July 15, 1988*, University of Dayton Research Institute, Dayton, Ohio.
10. T. A. Wittstruck et al., "Solid Hydrates of Some Halomethanes," *Journal of Chemical Engineering Data*, 6, 343-346 (1961).
11. G. V. Skorniyakov, "Operation of a Vortex Cooler," *Sov. Phys. (Tech. Phys. USA)*, 31 (11), 1332-1333, November 1986.
12. M. S. Bohn, "Heat Transfer and Pressure Drop Measurements in an Air/Molten Salt Direct-Contact Heat Exchanger," *Proceedings of the ASME 1989 Annual Solar Energy Division Conference*, San Diego, CA.

13. G. G. Bemer and G. A. J. Kalis, "A New Method to Predict Hold-Up and Pressure Drop in Packed Columns," *Trans. Instns. Chem. Engrs.*, 56, 200-204.
14. J. J. Stichlmair et al., "A General Model for Prediction of Pressure Drop and Capacity of Countercurrent Gas/Liquid Packed Columns," *Gas Separation and Purification*, 3, 19-28.

Internal Distribution

- | | |
|---------------------|--------------------------------------|
| 1. T. D. Anderson | 14. M. Olszewski |
| 2. R. S. Carlsmith | 15. A. E. Ruggles |
| 3. W. G. Craddick | 16. A. C. Schaffhauser |
| 4. J. B. Drake | 17. M. Siman-Tov |
| 5. D. M. Eissenberg | 18. T. K. Stovall |
| 6. W. Fulkerson | 19. M. J. Taylor |
| 7. J. A. Getsi | 20-25. J. J. Tomlinson |
| 8. J. E. Jones Jr. | 26. C. D. West |
| 9. L. Jung | 27. ORNL Patent Office |
| 10. R. J. Kedl | 28. Central Research Library |
| 11. M. A. Kuliasha | 29. Document Reference Section |
| 12. W. R. Mixon | 30-31. Laboratory Records Department |
| 13. F. R. Mynatt | 32. Laboratory Records (RC) |

External Distribution

33. Daniel M. Blake, Branch Manager Materials Research, Solar Energy Research Institute, 1617 Cole Boulevard, Golden, CO 80401
34. S. R. Bull, Solar Energy Research Institute, 1617 Cole Boulevard, Golden, CO 80401
35. Kevin Drost, Battelle Pacific Northwest Laboratories, P. O. Box 999, Battelle Boulevard, Richland, WA 99352
36. Russ Eaton, Advanced Utility Concepts Division, U.S. Department of Energy, CE-142, Forrestal Building, 1000 Independence Avenue, Washington, D.C. 20585
37. D. E. Gound, Program Manager, Research Management Branch, U.S. Department of Energy, ORO, Box 2001, Oak Ridge, TN 37831-8611
38. Landis Kannberg, Battelle Pacific Northwest Laboratories, P. O. Box 999, Battelle Boulevard, Richland, WA 99352
39. Kurt W. Klunder, Director, Office of Energy Management, Office of Utility Technology, U.S. Department of Energy, CE-14, Forrestal Building, 1000 Independence Avenue, Washington, D.C. 20585
40. George Manthey, DOE, Oak Ridge Operations, P. O. Box E, Oak Ridge, TN 37831
41. Veronika Rabl, Electric Power Research Institute, 3412 Hillview Avenue, P. O. Box 10412, Palo Alto, CA 94303
42. Eberhart Reimers, Advanced Utility Concepts Division, U.S. Department of Energy, CE-142, Forrestal Building, 1000 Independence Avenue, Washington, D.C. 20585
43. Robert L. San Martin, Office of Utility Technology, U.S. Department of Energy, CE-10, Forrestal Building, 1000 Independence Avenue, Washington, D.C. 20585
44. Chang W. Sohn, Energy Systems Division, U.S. Army Construction Engineering Research Laboratory, Corps of Engineers, Box 4005, Champaign, IL 61824-4005
45. R. D. Wendland, Project Manager, Thermal Storage Technology, Electric Power Research Institute, 3412 Hillview Avenue, P. O. Box 10412, Palo Alto, CA 94303

- 46. Office of Assistant Manager for Energy Research and Development, Department of Energy, ORO, Oak Ridge, TN 37831
- 47-58. Given distribution as shown in DOE/TIC-4500 under Category UC-202 (Thermal Energy Storage)